EUROPEAN FUSION DEVELOPMENT AGREEMENT

EFDA–JET–PR(02)23

E. Joffrin, C.D. Challis, G.D. Conway, X. Garbet, A. Gude, S. Guenter, N. C. Hawkes, T.C. Hender, D. Howell, G.T.A. Huysmans, E. Lazzaro, P. Maget, M. Marachek, A.G. Peeters, S.D. Pinches and S. Sharapov

Internal Transport Barrier Triggering by Rational Magnetic Flux Surfaces in Tokamaks

Internal Transport Barrier Triggering by Rational Magnetic Flux Surfaces in Tokamaks

E. Joffrin[1], C.D. Challis[2], G.D. Conway[3], X. Garbet[1], A. Gude[3], S. Guenter[3], N. C. Hawkes[2], T.C. Hender[2], D. Howell[2], G.T.A. Huysmans[1], E. Lazzaro[4], P. Maget[1], M. Marachek[3], A.G. Peeters[3], S.D. Pinches[3], S. Sharapov[2], and contributors to the EFDA-JET workprogramme*

[1]Association Euratom-CEA , Cadarache, F-13108, France.
[2]Euratom/UKAEA Fusion Association, Culham Science Centre, Abingdon, Oxfordshire, OX14 3DB, UK.
[3]Max-Planck-Institut fur Plasmaphysik, Euratom Association, 85748, Garching Germany.
[4]Istituto di Fisica del Plasma del CNR, Assoc. Euratom-ENEA-CNR per la Fusione, 20125 Milan Italy.
** See annex of J. Pamela et al, "Overview of Recent JET Results and Future Perspectives", Fusion Energy 2000 (Proc. 18th Int. Conf. Sorrento, 2000), IAEA, Vienna (2001).*

Preprint of Paper to be submitted for publication in
Nuclear Fusion

ABSTRACT.
The formation of Internal Transport Barriers (ITBs) has been experimentally associated with the presence of rational q-surfaces in both JET and ASDEX Upgrade. The triggering mechanisms are related to the occurrence of magneto-hydrodynamic (MHD) instabilities such as mode coupling or fishbone activity. These events could locally modify the poloidal velocity and increase transiently the shearing rate to values comparable to the linear growth rate of ITG modes. For JET reversed magnetic shear scenarios, ITB emergence occurs preferentially when the minimum q reaches an integer value. In this case, transport effects localised in the vicinity of zero magnetic shear and close to rational q values may be at the origin of the ITB formation. The role of rational q surfaces on ITB triggering stresses the importance of q profile control for advanced tokamak scenario and could assist in lowering substantially the access power to these scenarios in next step facilities.

1. INTRODUCTION

In recent years, the performance in terms of confinement and fusion yield in tokamaks devices (DIII-D [1], JT60-U [2], TFTR [3], Tore Supra [4], ASDEX [6] and JET [5]) has been significantly increased by forming a core region of reduced anomalous transport called Internal Transport Barrier (ITB). ITBs are generally associated with strong ExB shear flow [7], small or negative magnetic shear ($s = r/q\ dq/dr \sim 0$ or <0) [8] and turbulence suppression [9]. To extrapolate these improved regimes to larger size tokamaks and reactors with lower heating power density from external sources, it is essential to determine the minimum required power to access and sustain these regimes. Therefore, the triggering conditions to form an ITB need to be identified. In addition, the understanding of ITB triggering mechanism will assist the ultimate goal of actively controlling the onset, duration and confinement resulting from the formation of ITBs in advanced tokamak plasmas.

In the last two years, it was identified in JET [10], ASDEX Upgrade [11] and other devices (JT-60 [12], DIII-D [13], T10 [14], TFTR [15] RTP [16]) that low order rational q-surfaces are playing a key role in the internal transport barrier (ITB) formation for both reversed and low positive magnetic shear. This variety of magnetic central shear is usually obtained in the plasma current ramp-up using various combination of heating schemes. In JET, for example, low positive shear target q profiles (also named optimised shear (OS) discharges [5]) are produced without any heating or with small level of Ion Cyclotron Resonance Heating (ICRH) power. Strong reversed magnetic shear profiles are formed by pre-heating the plasma with Lower Hybrid Current Drive (LHCD) [17]. The combined effect of off-axis current drive and electron heating by the lower hybrid wave can sometimes result in very large value of the central safety factor q_o [18]. This tailoring of the target current density profile has made possible the study of the ITB triggering mechanism for different value of the magnetic shear in the plasma centre [19]. At a macroscopic level, the access power to the ITB regime is experimentally influenced by the different classes of q profile. For low positive shear, the access power roughly scales as $5.B_T$ [5]. However, for negative central shear q profile (i.e. when a zero shear point exists in the plasma), the access power to the ITB regime can be

much lower [20]. Since the ITB triggering is linked with low order rational q-surfaces for both classes of q profiles, this is suggesting that the physics of the ITB triggering mechanism is linked with the physics properties of rational q-surfaces. Therefore, the study of this physics could be decisive in predicting the access power to the ITB regime for larger size tokamaks.

This paper first summarises the experimental evidence demonstrating the relation between rational surfaces and ITB emergence. These analyses are showing in particular that the ITB triggering mechanisms are related to the specific transport and magneto-hydro-dynamic (MHD) properties of rational q-surfaces. The influence of the rational q-surfaces on the access power to the ITB regime is also described for both reversed and low positive magnetic shear. In the next sections, the modelling of the MHD mechanism for ITB formation is presented for both ASDEX Upgrade reversed magnetic shear and JET low positive magnetic shear scenario. The creation of ITB in the JET reversed magnetic shear scenario is discussed in the last section. Transport property of rational q-surfaces is put forward as a possible explanation for the emergence of ITBs at $q_{min} = 2$ or 3 on the basis of the recent theoretical works on rational surface rarefaction.

2. RELATION BETWEEN RATIONAL SURFACE AND ACCESS POWER TO THE ITB REGIME

The link between rational surfaces and ITBs have now been observed in a large number of devices. The RTP tokamak had first reported the link of rational surface and local improved confinement structure [16]. In larger devices such as DIII-D [13] the role of rational surfaces has also been observed in reversed magnetic shear at power density comparable to that used in JET. At higher power density, the triggering mechanism related to rational is generally not seen which is consistent with what is observed in JET. In JT60, the role of rational has also been reported and double barriers linked with an integer rational recently have been observed [21]. In TFTR, the ERS mode ITB is located in the vicinity of the q=2 surface [15]. In addition, stellarator have also recently described the link between between ITBs and rationals [22]. It seems therefore that the role of rational in the ITB physics is quite fondamental.

In JET and ASDEX Upgrade, two independent experimental studies have confirmed that rational surface are at the origin of the internal transport barrier for both low positive and strongly reversed shear.

In ASDEX Upgrade, the emergence of ITB in reversed magnetic shear has been related to the presence of fishbone on the q=2 surface [23]. The physics of the ITB triggering mechanism in this device is presented in the next section of this paper.

In JET, internal transport barriers have been observed in correlation with integer q surface such as q=1, 2 or 3 for low positive shear discharges [24]. It was also demonstrated that the creation of these ITBs at constant power is closely linked to the time when the main heating is applied. As the target q profiles evolves (i.e. when q profile decreases) more power is required to trigger an ITB. Figure 1 illustrates this point on a large database of 3.4T low reversed magnetic shear pulses. At

this magnetic field and at the lowest heating power at which an ITB is observed (20MW) ITB can only be formed in a narrow range of q profile when qo is close to 2. As the target qo is reduced and the q=2 surface widens and more power is required to form an ITB. This illustrates that the power access to form an ITB can be minimised by optimising the current density profile. The control of the q profile is therefore a very important asset in the access to the ITB regime. In larger devices, where the power density from additional heating is expected to be relatively small, this feature may be decisive in creating an ITB in the advanced tokamak scenario.

More recent experiments have extended this analysis to reversed magnetic shear q profile [19] using the LH power in the pre-heat. The first observations were that ITB could be triggered below the access power determined for low positive magnetic shear independently from the power level. Figure 2a shows the effect of the main heating power (NBI + ICRH) on the ITB formation. Here, t_{heat} is the time when the main heating power is injected. This time also defines the so-called "target" q profile. As the power increases, the emergence of the ITB determined by the JET ITB criterion [25] is delayed. This is consistent with the current diffusion during the main heating phase. At high power, the current diffusion rate is slower and the q=2 surface appears later. The determination of q profiles from motional Stark effect (MSE) and infrared polarimetry indicates that the ITB emergence time coincides with the time when qmin reaches 2 (figure 2b). The fact that the ITB is triggered when qmin reaches 2, confirms again that the access to the ITB regime is not clearly linked to the input power, but rather to an optimum q profile when the main heating is applied. The zero shear point appears to be a favourable point for the ITB triggering when it reaches an integer surface. Once the ITB triggered, the ExB shear flow develops and its location follows the integer q-surface. At this stage, the minimum input power depends essentially on the power required to maintain the plasma in this bifurcated state.

The presence of the q=2 surface at q_{min} is experimentally confirmed by the detection of Alfvèn cascades as q_{min} reaches q=2. Alfvèn modes are generally excited by energetic ions accelerated by the ICRH wave. A detailed theoretical interpretation has demonstrated that these Alfvèn cascades with upward frequency sweeping occur when qmin passes a rational magnetic surface [26]. The simultaneous excitation of n=2 to n=6 Alfvèn cascades (as in figure 3a) can only occur when the condition m-n. $q_{min}(t)=0$ and is fulfilled as q_{min} passes q=2 as already suggested by the equilibrium reconstruction. Using this technique, a data set of about 20 discharges with at least 2MW of ICRH power have been analysed and the time of the cascade onset is correlated with the emergence time of the ITB as detected by the JET ITB criterion [25]. The remarkable correlation (figure 3b) between these two times shows that Alfvèn cascades can now be used as a very efficient diagnostic for the determination of the q profile at the time the ITB is formed. It should be pointed out that Alfvèn cascades are in general not detected when the ICRH power is less than 2MW, even though an ITB is still produced. This indicates that the fast ions produced by the ICRH wave are not playing a major role in the ITB triggering process in JET.

The importance of rational q-surfaces in the formation of ITBs reinforces the need for q profile

control for advanced tokamak operation. The access power to the ITB regime appears to be closely linked to the local action of rational q-surfaces on ExB shear flow. In the following sections, the detailed analyses of three cases (ASDEX Upgrade low magnetic reversed shear, JET low positive magnetic shear and JET reversed magnetic shear scenario) examine the possible mechanism leading to the formation of the ITB at the rational surface location.

3. ITB TRIGGER MECHANISMS IN ASDEX UPGRADE

Recent observations [11, 23] have indicated that the formation of internal transport barriers in ASDEX Upgrade are preceded by fishbone activity on q-surfaces such as q=2, i.e. oscillation of the internal kink driven by the fast ion population (figure 4). The mechanism by which this happens relies on the interaction between these fast ions with the kink distortion. Due to the perturbed magnetic field, the fast ions are expelled radially leading to a local enhancement of the radial electric field.

The time evolution of the fast ion radial current has been computed by the HAGIS code [27] evolving the distribution of energetic ions as they interact with the kink mode. The radial magnetic structure of the mode is inferred from experimental data from the electron cyclotron emission (ECE) and magnetic diagnostics. The velocity distribution of fast ions is specified as a slowing down distribution from the injection energy of 60keVwith a volume averaged β for fast particles.

From this radial current, the effective radial electric field is inferred. Rze poloidal rotation and sheared flow evolutions are deduced from the equation of motion and force balance equations respectively. A comparison of the shearing rate calculated for ASDEX Upgrade parameters indicates that fishbones with a sufficiently high repetition frequency (typically above the effective collision time scale) give shearing rate comparable with estimates of the linear growth rate of ion temperature modes (ITG) modes. Although, some effect like the particle sources are not included in this model, fishbones can thus be a suitable candidate for the triggering of ITBs.

This work demonstrates that the radial current of fast ions expelled by fishbones can lead to the generation of shear flow. In fusion plasma with strong fast alpha particle pressure, this effect may turn out to play a role in the production of ITBs.

4. TRIGGER MECHANISM IN LOW POSITIVE MAGNETIC SHEAR IN JET.

In JET, a recent experimental study has shown that the ITB emergence is well correlated with an external kink mode destabilised as an integer q surface (q=4, q=5 or q=6) enters the plasma in the current ramp-up [24]. Since ITBs are formed in the vicinity of internal integer q surfaces, toroidal mode coupling has been put forward as the most plausible candidate mechanism to explain the link between the edge MHD occurrence and the ITB emergence time. Simulations with the CASTOR code have confirmed that strong mode coupling can occur between the edge MHD mode and the internal q surface. The destabilisation of the MHD at q=2 or q=3 by the coupling process could provide a locally enhanced sheared flow by ‘mode braking’, and act as a trigger for the ITB formation.

To examine this hypothesis and evaluate the effect of mode braking on plasma flow, the model shown below makes use of the linearised MHD equations including toroidal effect between two resonant layers. The resonance layers are supposed to be in the non-linear regime and the plasma response is determined by diamagnetism and transverse transport (diffusion and viscosity). These equations are solved together with the evolution equations for the plasma flow in both toroidal and poloidal directions.

The system of coupled equations between the poloidal and toroidal rotation and the growth rates (or Δ') of the edge and internal modes is calculated from the variational principle for a given n number (here n=1). The coupled equation for the evolution of the island width W (normalised to the minor radius) and phase ϕ are expressed for each resonant surface as [28]:

$$R_b \frac{\partial W_b}{\partial t} = \Delta'_b + \frac{C}{s_b} \frac{W_e}{W_b^2} \cos(\varphi_e - \varphi_b) \quad \text{and} \quad R_e \frac{\partial W_e}{\partial t} = \Delta'_e + C\, s_b \frac{W_b}{W_e^2} \cos(\varphi_e - \varphi_b)$$

$$\frac{\partial \varphi_b}{\partial t} = k_\theta + V_b^* + k_\theta V_{\theta b} + k_\varphi V_{\varphi b} + \frac{C}{\kappa_b \cdot s_b} W_e^2 W_b \sin(\varphi_e - \varphi_b)$$

$$\text{and} \quad \frac{\partial \varphi_e}{\partial t} = k_\theta + V_e^* + k_\theta V_{\theta e} + k_\varphi V_{\varphi e} - \frac{C \cdot s_b}{\kappa_e} W_b^2 W_e \sin(\varphi_e - \varphi_b)$$

In these equations, the index "b" denotes the quantities at the barrier location and "e" at the edge. C is the coupling parameter and is approximated by C~a/R. R_b, Re and s_b , s_e are respectively the resistive times and the magnetic shears at each resonant surface. Finally κ_b (and κ_e) are given in [29]: $\kappa_b = 88 D \beta \left(\frac{qR}{s_b.a}\right) \frac{1}{k_\theta^2 a} c_s$, using the Gyro-Bohm approximation for the diffusion coefficient D and where cs is the sound speed.

The equation of motion for the plasma in the toroidal and poloidal direction at the location of the rational surface are described by:

$$m\, n \frac{\partial V_\theta}{\partial t} = P_\theta - m\, n\, \nu_{neo} (V_\theta - k_{neo} V^*) \text{ and}$$

$$m\, n \frac{\partial V_\varphi}{\partial t} = P_\varphi - m\, n \frac{1}{r} \frac{d}{dr}\left(r\mu \frac{dV_\varphi}{dr}\right) + P_{beam}$$

where $V^* = \frac{2T_i}{e\, a\, B_o}$, $\nu_{neo} = \nu_{ii}\, q_2\, (r/a)^{3/2}$, μ is the viscosity and k_{neo} ~1.17 in the collisionless regime. P_θ and P_φ are the poloidal and toroidal momentum per unit volume transferred to the plasma by the mode on the considered resonance layers. This momentum will act on the plasma over a spatial range determined by a form factor L such that $\int L(\rho).d\rho = 1$ where $\rho = r/a$ is the normalised radius. This function L depends on the model employed outside the island separatrix. In the present calculation, the behaviour of the flow shear away from the separatrix of the island is described as in reference [30] taking into account the diamagnetic effect in the vicinity of the island. In this case, the function L is described by an exponential and the typical width of the region where the plasma

is entrained by the island is estimated to be:

$$\lambda = \rho_s \cdot \sqrt{\frac{\mu}{D}}$$, where ρ_s is the ion Larmor radius.

In steady state and without mode coupling, one can note from the above equations that the plasma at the rational surface will rotate with the diamagnetic frequency in the poloidal direction and with the neutral beam momentum P_{beam} in the toroidal direction.

These equations are integrated over the plasma volume and then solved using, the q = 2 surface as the internal surface and the q = 4 as external surface. The edge mode on the latest is artificially destabilised by an increase of its Δ_e'. This choice reproduces the observed experimental situation where the external mode on the q = 4 surface is destabilised by an excess of edge current and couples with the q = 2 surface at the ITB location. Figure 5 shows the behaviour of the simulated poloidal and toroidal velocity with time using typical plasma parameters ($T_e = 2$keV, $B_T = 2.6$T, $n_e = 2\times10^{19}$ m^{-3}). The edge pertubation is simulated by an increase of Δe' from 0 to 2, corresponding to an edge perturbation $\underline{B}_\theta/B_\theta \approx 10^{-3}$. The poloidal velocity starts to oscillate with an amplitude of about 400m/s and a frquency of a few Hz. This oscillation indicates that the two resonant surfaces are not locked to each other but are in an intermediate state where the edge mode starts to brake the growing q = 2 island. The change in toroidal rotation is relatively modest and the island at the q = 2 surface increases to a size of less than 2cm. This is making difficult the detection of this island by magnetic measurements on the wall of the vacuum vessel. However, the effective change of poloidal rotation (~200m/s) imposed by the q = 2 island will strongly modify the shear flow outside the island separatrix. Using the cylindrical definition of Hahm and Burrell [31], the shear rate is defined for the case of low magnetic shear and sharp electric field gradients:

$$\gamma_E \approx \left|\frac{1}{r}\left(\frac{Er}{B_o}\right)\right| \approx \left|\frac{d}{dr}V_\theta\right| \approx \frac{V_\theta}{\lambda} \approx 5\times10^4\ s^{-1}$$

For this example, the shearing rate can be compared to the linear growth rate of ion tempearature gradient (ITG) mode:

$$\frac{\gamma_{lin}}{k_\theta \cdot \rho_s} = \frac{V_{th}}{\sqrt{a.R}} = 2.2\times10^5\ s^{-1}$$

showing that mode braking is capable of triggering an ITB by inducing strong local shearing rate exceeding the linear growth rate of ITG turbulence (lin) for k .s of the order of 0.2.

Experimentally, the poloidal flow is not yet routinely measured in JET although recent results look encouraging [32]. However in TFTR [15] and also in ASDEX Upgrade [33], poloidal rotation measurements have indeed detected, at the time of the ITB formation, sharp local velocity decrease far above the neoclassical value. In both experiments, this drop is very localised, typically over a few centimeters. These preliminary measurements suggest that local braking of the plasma flow occurs possibly as a result of some MHD events as described by the model presented above.

The model also indicates that the coupling process strongly relies upon the strength (or $\Delta e'$) of the external pertubation. This strength depends on the amount of edge current at the time the rational edge q is reached, and therefore, the current diffusion process in the current ramp-up plays an essential role. By replacing the external magnetic perturbation from the edge kink mode by an imposed perturbation provided by saddle coils, for example, it may be possible to use the property of rational q surface to actively trigger the emergence of the ITB. Such an experiment would be the ultimate demonstration that rational surface can act locally on the shear flow and trigger an ITB.

4. TRIGGER MECHANISM IN REVERSED MAGNETIC SHEAR IN JET.

In reversed shear q profile the emergence of ITBs has also been confirmed to correlated with $s = 0$ reaching a rational magnetic q-surface such as 2 or 3 as explained in section 1. Figure 6a shows the evolution of the ρ^*_T criterion [25] as the zero shear point reaches the rational surface $q = 2$ (detected by the observation of an Alfven cascade). From this point, two internal transport barriers develop at two different radial locations: one in the negative shear and the other in the positive shear region. The two ITBs appear to follow the two $q = 2$ surfaces on each side of q_{min}. This behaviour is observed in a systematic way and has been described in more details in reference [19]. Also, it cannot be explained only by non global turbulence simulations or most of the transport models since they are not assigning any special role to resonant surfaces. In addition, no MHD activity has been in general observed at the time of the ITB formation in contrast to the low positive shear case.

On the other hand, the argument of the rarefaction of flux surfaces already put forward by previous authors [34, 35] could provide a possible explanation for this behaviour. Although fluid simulations [36] are showing the importance of negative magnetic shear for the stabilisation of high wave number ITG modes, sharp barrier could develop at the location of zero magnetic shear in the vicinity of low order rational surface [35]. The rarefaction of resonant surfaces around these points can create gaps which are not balanced by an increase of the turbulence radial correlation length (typically one centimeter in JET). Once the ITB is produced, its location and width are maintained by the rotational shear.

The width of the gap between rationals q surfaces scales as the square root of the Larmor radius and depend on the curvature of the q profile as:

$$d_{gap} = \left[\frac{2.q_{min}.\rho_i}{n.r_{min}.q''_{min}} \right]^{\frac{1}{2}}.$$

When this gap width exceeds the turbulence correlation length L_c (scaling like ρ_i for gyro-Bohm scaling), simulations are suggesting that an internal transport barrier can be formed [33]. In this expression, it should be noted that the q profile shape (i.e. the second derivative of q) is the dominant factor in d_{gap} since ρ_i scales as $T_e^{1/2}/B_o$ which is itself roughly constant with the plasma radius r.

To examine this idea, the evolution of the gaps between resonant surfaces has been computed for Pulse No: 51579. The experimental q profile shape is scanned across the $q = 2$ surface and the

gaps calculated for toroidal and poloidal number up to 80 (figure 6b), i.e. $k_\theta.\rho s \sim 0.5$. When the q = 2 surface is reached a large gap opens and then two gaps on each side of the q = 2 surfaces propagating on each side of qmin. Shortly after, it appears that high n and m resonant surfaces are developing in between these two gaps, dividing them and making possible the formation of two internal transport barriers at two different radial locations as observed by the experiment. This indicates that the evolution of rational surfaces around a low integer q-surface could be at the origin of the formation of the two observed ITBs.

In general, no strong MHD activity is observed in reversed shear plasmas apart from the Alfven cascades. However, the presence of MHD activity occurring on the two q = 2 surfaces cannot be completely ruled out. After the q = 2 surface has reached a rational, the two q = 2 surfaces on each side of qmin could coupled non-linearly as the q profile decreases as a result of the current diffusion. In presence of a sheared flow, the internal surface remains at the same rotation frequency than the external surface and modifies locally the E×B shear flow at the innermost q = 2 surface. This can favour the creation of an ITB in the negative magnetic shear region with the same process described in section 3 [37]. Another theoritical idea is suggesting that electromagnetic turbulence might be responsible for a flow generation close to rational q values [38]. The suggested picture of plasma turbulence involves variation of temperature and density profiles induced by electromagnetic fluctuations which could modify the evolution of the radial electric field. This explanation does receive some supports from the simulations but would require specific turbulence measurements to be demonstrated.

In summary, the role played by rational q surfaces in reversed shear plasmas can be explained by several mechanisms. It is not yet clear which mechanism is acting to trigger the ITB. In any event, the role played by rational q surfaces supports the recent efforts undertaken to actively control the q profiles to trigger and sustain the ITB regime in tokamak [39].

CONCLUSIONS

The formation of ITBs in many tokamaks (JET, ASDEX Upgrade, JT-60, DIII-D) and also stellarators is closely related to rational surfaces and in particular to integer surfaces. This relation has some profound impacts on the power required to trigger an ITB. This paper has demontrated that the processes linked with rational q-surfaces physics (MHD and transport) can lower the access power significantly in both low positive and strongly negative magnetic shear.

In ASDEX-Upgrade, fast particles seem to play a dominant role through the generation of fishbone activity at the rational surface. The specific role of fast particle could be of importance in a burning plasma with strong alpha particle pressure.

On the other hand, the role of fast particle is not observed in JET. For low positive magnetic shear plasma, coupling mode processes can account for the enhancement of shear flow at the location of the rational surface and produce the ITB.

This suggest that the poloidal flow can be controlled by magnetic braking using an external

magnetic perturbation. In strongly reversed shear, it appears that the zero shear point is the most favorable point for triggering an ITB as it reaches an integer value. This point is demonstrated experimentaly by the analysis of Alfvèn cascade which can now be used as a diagnostic. From this point two ITBs can be triggered on each side of q_{min} and follow the two integer surfaces. The rarefaction of rational surfaces around an integer at low shear could provide an possible explaination for that behaviour. Other proposed candidate mechanisms are all related to the specific properties of rational q-surfaces, either transport or MHD. The common denominator of all the triggering mechanisms are in any case strongly suggesting that the active and fine control of the current density profile will be an extremely important tool for accessing the ITB regime in next step machines.

The analysis of the ITB triggering mechanisms in JET and ASDEX-Upgrade has demonstrated that the physics properties of resonant q-surfaces are essential for the understanding the physics of ITB formation. Ultimately the knowledge and the control of the triggering conditions to form an ITB will assist in minimising the required input power to access ITB regimes in advanced tokamak plasmas for larger size devices.

REFERENCES

[1]. B. W. Rice et al., Phys. Plasmas **3** (1996) 1983

[2]. T. Fujita et al., Proc. in Fusion Energy (16th Int. Conf. Montréal 1996), IAEA, Vienna, **Vol. I** (1997) 227.

[3]. F.M. Levinton et al., Phys. Rev. Lett. **75** (1995) 4417

[4]. Equipe Tore Supra, presented by X. Litaudon, Plasma Phys. Control. Fusion **38** (1996) A251.

[5]. C. Gormezano, et al., Plasma Phys. Control. Fusion, 41, (1999) B367. See also: A. Becoulet et al., Plasma Phys. Control. Fusion **43** (2001) A395-A406.

[6]. R.C. Wolf, et al, in Fusion Energy, (Proc. 17 th Int. Conf. Yokohama 1998), IAEA, Vienna, **Vol. II** (1999) 773.

[7]. K.H. Burrell, Phys. Plasma **4** (1997) 569.

[8]. S.C. Guo and J. Weiland, Nuc. Fusion **37** (1997) 1095.

[9]. G.D. Conway, et al., Phys. Rev. Lett. **84** (2000) 1463.

[10]. C.D. Challis et al., Plasma Phys. Control Fusion, **43** (2001) 861

[11]. S. Guenter et al, Proc. 28 th European Physical Society Conf. on Control. Fusion and Plasma Physics, Madeira, **25A** (2002) P1.006.

[12]. Y. Koide et al., Phys. Rev. Lett **72** (1994) 3662

[13]. C.M. Greenfield, et al, in Fusion Energy (Proc. 17th Int. Conf. Yokohama 1998, IAEA, Vienna, **Vol. II** (1999) 69.

[14]. K. A. Razumova et al., 19 th Fusion Energy Conf., Lyon, France (2002) IAEA-CN-94/ EX/ P3-03.

[15]. M. Bell, et al., Plasma Phys. and Control. Fusion, **41**, (1999) A719

[16]. G.M. D. Hogeweij et al., Nuc. Fusion **38** (1998) 1881

[17]. J. Mailloux et al., Phys. Plasmas **9** (2002) 2156-2164.
[18]. N.C. Hawkes et al., Plasma Phys. Control Fusion **44** (2002) 1155.
[19]. E. Joffrin et al., Plasma Phys. Control Fusion **44** (2002) 1739
[20]. C.D. Challis et al., Plasma Phys. Control Fusion, (2002),
[21]. S. V. Neudatchin et al., 19 th Fusion Energy Conf., Lyon, France (2002) IAEA-CN-94/ EX/ P2-06.
[22]. C. Alejaldre et al., 19 th Fusion Energy Conf., Lyon, France (2002) IAEA-CN-94/EX/ OV /4-4
[23]. S. Pinches et al., Proc. 28 th European Physical Society Conf. on Control. Fusion and Plasma Physics, Madeira, **25A** (2002) P1.008.
[24]. E. Joffrin, et al., Nuc. Fusion **42** (2002) 235-242.
[25]. G. Tresset, et al., Nuc. Fusion **42** (2002) 520
[26]. S.E. Sharapov, D. Testa, et al., Physics Letters **A 289** (2001) 127.
[27]. S. D. Pinches et al., Computer Physics Communications **111** (1998) 133
[28]. D. Edery and A. Samain, Plasma Physics and Controlled Fusion **32** (1990) 93
[29]. A. Samain, Plasma Physics and Controlled Fusion **26** (1984) 731
[30]. J. W. Connor et al., Phys. Plasma **8** (2001) 2835
[31]. T.S. Hahm and K.H. Burrell, Phys. Plasma **2** (1995) 1648.
[32]. F. Sattin et al., Proc. 28 th European Physical Society Conf. on Control. Fusion and Plasma Physics, Madeira, **25A** (2002) P1.096.
[33]. S. de Pena Hempel, et al., Proc. 25 th European Physical Society Conf. on Control. Fusion and Plasma Physics, Praha, **22C** (1998) 484.
[34]. F. Romanelli and F. Zonca, Phys. Fluids **B 5**, 4081 (1993).
[35]. X. Garbet et al., Physics of Plasma, **8**, (2001) 2793.
[36]. X. Garbet et al., 19 th Fusion Energy Conf., Lyon, France (2002) IAEA-CN-94/EX/ TH/ 2-1
[37]. P. de Vries, private communication.
[38]. A. Thyagaraja, Plasma Phys. Control. Fusion **42** (2000) B255
[39]. D. Mazon et al., Plasma Phys. Control. Fusion **44** (2002) 1087

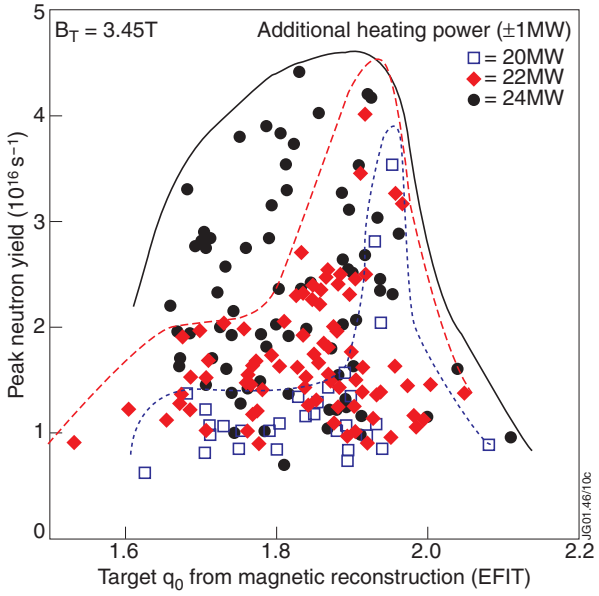

Figure 1:Neutron yield versus qo for a 3.4T database of discharges with three different input powers. The curves envelope three different domains of input power. At 20MW (open squares) strong barriers can be formed in a narrow range of target q when qo is close to 2 At higher powers, 22MW (diamonds) 24MW (circles, the domain of existence is less sensitive to the q profile.

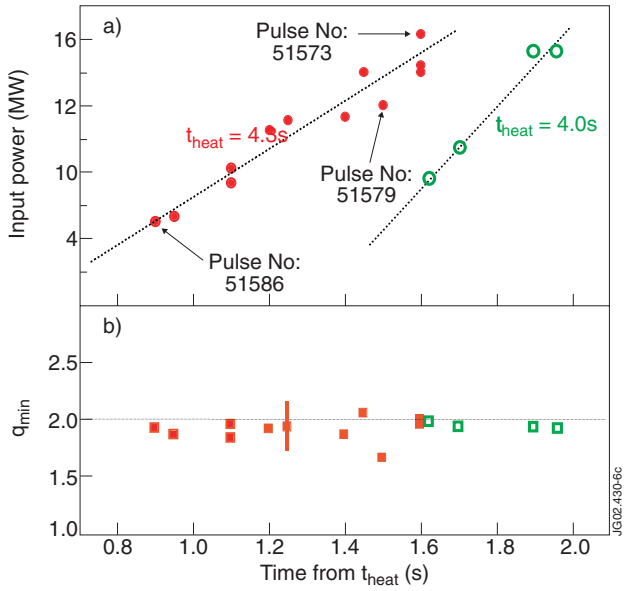

Figure 2: Emergence time of the ITB in strongly reversed magnetic shear. a) The ITB triggering does not appear to depend on the input power level. b) However it is correlated with q_{min} reaching the q=2 surface. (t_{heat} is the time when the main heating is applied). This indicate that the ITB formation is sensitive to the q profile but not to the input power level.

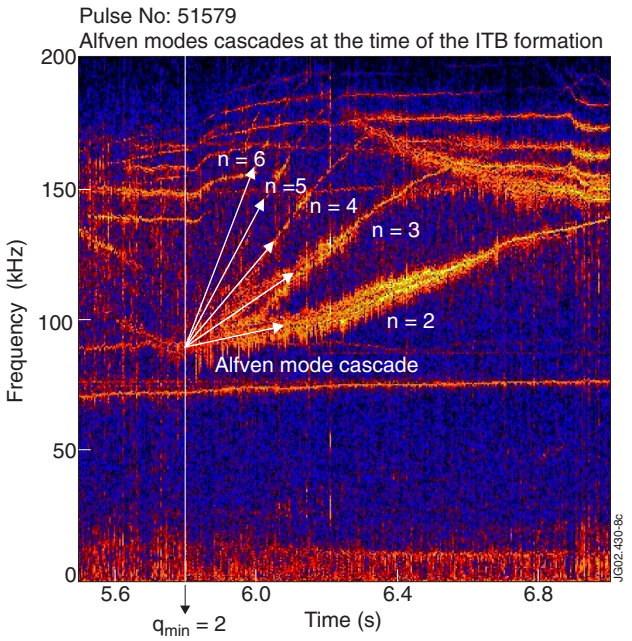

Figure 3a: Spectrogram of an Alfvèn mode cascade observed at 5.8 at the time of the ITB formation from the signal of high frequency coils installed in the JET vaccum vessel (Pulse No: 51579 indicated on figure 2). The simultaneous excitation of the Alfvèn wave cascade with toroidal mode number from 2 to 6 can occur only if qmin passes an integer value at this very moment (q=2 in this case).

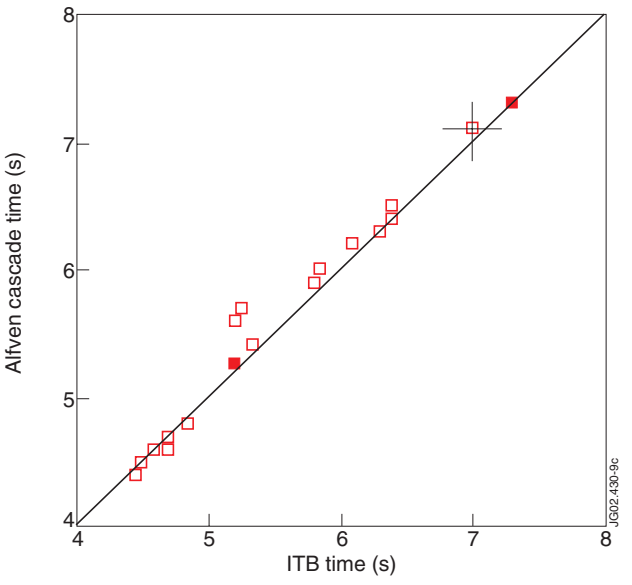

Figure 3b: Correlation between the emergence time of the ITB from the ITB criterion [25] and the Alfvèn cascade time. This remarkable correlation makes the Alfvèn cascades a useful diagnostic for determining the time when qmin passes a rational flux surface.

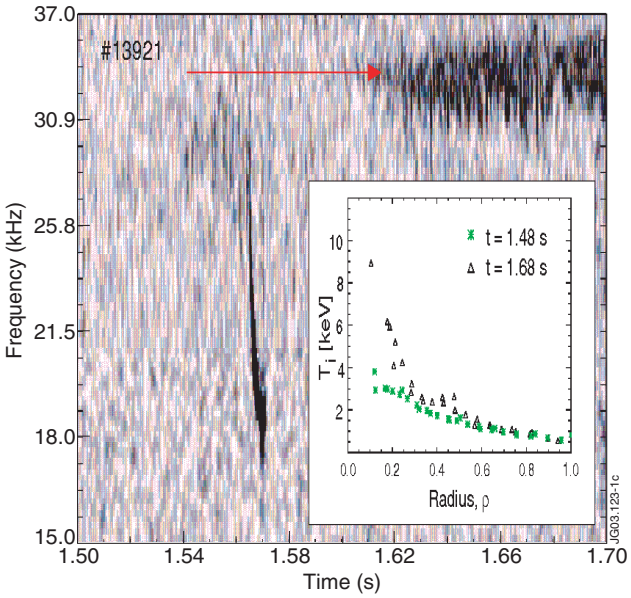

Figure 4: Spectrogram of magnetic fluctuations showing the fishbone oscillations on q=2 at the start of the ITB in ASDEX Upgrade. The inset illustrates the ion temperature profil change before and during the fishbone activity.

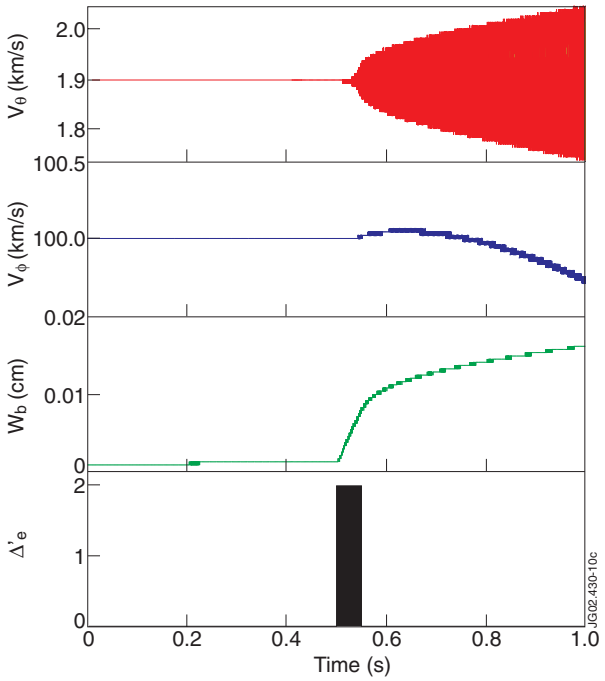

Figure 5: Simulation of the poloidal and toroidal flow at the q=2 surface when an edge perturbation grows at the q=4 surface at the edge (simulated by an increase of its Δ'). As coupling occurs (at t=0.5s), the island on q=2 grows, and the poloidal velocity starts to be strongly affected. The oscillations of V indicate that the two modes are not fully locked, but braking of the plasma flow do occur.

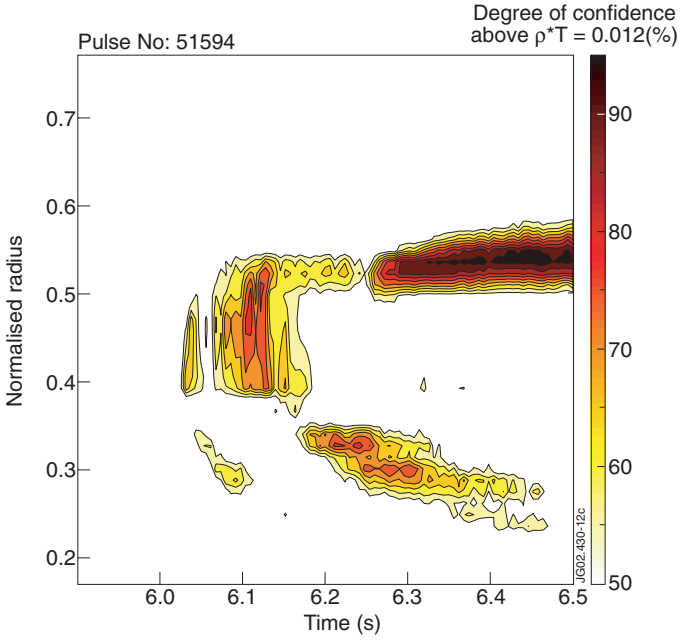

Figure 6a: ρ^*_T contours for Pulse No: 51594 (see figure 2) showing that two ITB can be created at two different radial position as qmin reaches the q=2 surfaces. The time when q_{min} passes the integer surface 2 is determined by the Alfvèn cascade analysis and is also indicated.

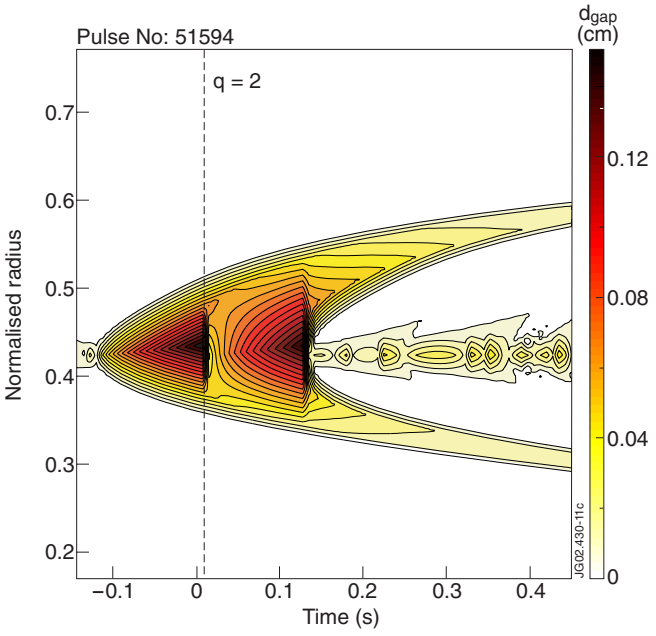

Figure 6b: Simulation of the gap (d_{gap}) between rational surfaces when the q profile evolves through the q=2 integer surface. Toroidal and poloidal number up to 80 are used in this example, corresponding to a value of $k_\theta \rho_i$ of the order of 0.5. This picture is in qualitative agreement with figure 6a and shows that two large gaps can open on each side of q_{min} and facilitate the de-correlation of the turbulence and the emergence of two ITBs.